

Long-Range Correlations in the Two-Dimensional Spin- $\frac{1}{2}$ Antiferromagnetic Heisenberg Model: A Quantum Monte Carlo Study

Efstratios Manoussakis and Román Salvador

Supercomputer Computations Research Institute, Florida State University, Tallahassee, Florida 32306

(Received 1 December 1987)

Using an extended version of Handscomb's Monte Carlo method we study the spin- $\frac{1}{2}$ quantum antiferromagnetic Heisenberg model on square lattices of various sizes. The calculated correlation length associated with antiferromagnetic order grows very rapidly as the temperature is lowered, suggesting an essential singularity. Our results are consistent with those recently observed by neutron scattering done on La_2CuO_4 .

PACS numbers: 75.10.Jm, 74.20.-z

The recently discovered high-temperature superconductors¹ exhibit interesting magnetic properties. The $\text{La}_2\text{CuO}_{4-y}$ material has a susceptibility anomaly at a Néel temperature T_N which is sensitive to the value of y , increasing from $T_N=0$ for $y=0$ to $T_N \approx 295$ K for $y=0.03$.² Subsequent neutron-scattering experiments³ show that the materials order antiferromagnetically and in a La_2CuO_4 single crystal there are instantaneous two-dimensional (2D) antiferromagnetic correlations⁴ exceeding 200 Å for $T \approx 200$ –300 K, with no average staggered magnetization. Neutron scattering⁴ and Raman scattering from magnon pairs⁵ provide a large value for the antiferromagnetic (AF) coupling $J \approx 10^3$ K.

There are theoretical studies which examine the possibility of superconductivity mechanisms originating purely from electronic degrees of freedom. In some of these studies the magnetic properties of the materials are one of the central points. A common point of departure is the Hubbard model in its strong-coupling limit.^{6,7} In this limit and at half filling this model is equivalent to the spin- $\frac{1}{2}$ antiferromagnetic Heisenberg model (AFHM)

$$H = J \sum_{\langle ij \rangle} \mathbf{S}_i \cdot \mathbf{S}_j, \quad (1)$$

where $\langle ij \rangle$ denotes nearest-neighbor unit cells in the Cu-O plane and \mathbf{S}_i is the spin operator of the conduction-band electron located at the i th cell. This model is expected to describe the dynamics of spin fluctuations in the undoped La-Cu-O material.

In this paper we simulate the quantum spin- $\frac{1}{2}$ AFHM (1) in 2D using Handscomb's method as it has been extended for antiferromagnets.⁸ We perform the calculation on various size lattices and measure among other quantities the spin-correlation function. The extracted correlation length $\xi(T)$ grows very rapidly as we lower the temperature. For the temperature varying from $\sim 0.7J$ to $\sim 0.4J$, ξ grows from ~ 1.5 to ~ 13 unit cells. The behavior of the correlation length suggests an essential singularity. The detailed behavior of the correlation function is different from that obtained by perturbative

renormalization-group analysis of the classical Heisenberg model. A dramatic growth of correlations is also revealed by the analysis of the neutron-scattering experiments⁴ on La_2CuO_4 at room temperatures. If we take the value of J of the order of 10^3 K, extrapolation of our results at $T \approx 200$ –300 K gives correlation lengths of the same magnitude as those observed.⁴

The Hamiltonian (1) can be written as⁸

$$-\beta H = (\beta J/2) \sum_{\langle ij \rangle} (h_{ij}^2 - h_{ij}) + \text{const}, \quad (2)$$

where $\text{const} = NJ/2$ (N = number of unit cells). The operator h_{ij} is equal to $S_i^+ S_j^- + S_i^- S_j^+$, and flips antiparallel spins and gives zero in the case of parallel spins. This Hamiltonian, when derived from the strong-coupling Hubbard model at half filling (see Ref. 7), describes processes in which the electron hops to a nearest-neighbor cell occupied by an electron of opposite spin, making the site doubly occupied momentarily, and in the final state both return either to the original configuration (h_{ij}^2 term) or to the one with spins exchanged (h_{ij} term).

Following Ref. 8, any observable \hat{O} can be calculated as

$$\langle \hat{O} \rangle \equiv \frac{\text{Tr}(\hat{O} e^{-\beta H})}{\text{Tr}(e^{-\beta H})} = \frac{\sum_{r=0}^{\infty} \sum_C \pi(C_r) \Omega(C_r)}{\sum_{r=0}^{\infty} \sum_C \pi(C_r)}, \quad (3a)$$

$$\pi(C_r) = (-1)^{r_1} \frac{(\beta J/2)^r}{r!} \text{Tr}(Q_{i_1} Q_{i_2} \cdots Q_{i_r}), \quad (3b)$$

$$\Omega(C_r) = \frac{\text{Tr}(\hat{O} Q_{i_1} Q_{i_2} \cdots Q_{i_r})}{\text{Tr}(Q_{i_1} Q_{i_2} \cdots Q_{i_r})},$$

where i_n denotes a link, $\langle ij \rangle$ for instance, and $Q_{i_n} = h_{ij}^2$ or h_{ij} . $C_r = \{i_1, i_2, \dots, i_r\}$ is a sequence of $r = r_1 + r_2$ operators and r_1 (r_2) is the number of h 's (h^2 's) in the sequence. If the h operators in C_r do not form closed loops the trace is zero. Hence for a square lattice the number of h 's in a string must be even and consequently $\pi(C_r)$ is nonnegative. The trace of any string of operators is the product of the traces of all the clusters. A cluster is a set

of lattice sites connected by operators. An isolated site is also a cluster (monomer). Given an operator sequence forming a cluster, we can construct either two possible states contributing to the trace or none. In the latter case the particular sequence is not allowed. The trace over the entire lattice is equal to either zero or 2^{n_c} (n_c = total number of clusters).

A Markov chain generating a distribution $\pi(C_r)$ of sequences C_r is the following. At each iteration of the random walk we can add or remove any number n_a or n_d of operators, respectively. We decide to add or delete an operator with equal probability. We select a given operator to be added with probability $1/4N$ and the specific location in a string with r operators with probability $1/(r+1)$. We remove a given operator with probability $1/r$. The acceptance probability for a transition from the state C_r having r operators to the state $C_{r'}$ having $r' = r + n_a - n_d$ operators and satisfying the detailed balance is given by

$$P(C_r \rightarrow C_{r'}) = \min \left[1, w \left(\frac{1}{4N} \right)^{r-r'} \frac{\pi(C_{r'})}{\pi(C_r)} \right], \quad (4)$$

where the factor $w = \frac{1}{2}, 2,$ or 1 , for $r=0, r'=0,$ or $r \neq 0$ and $r' \neq 0$, respectively.

We have tested our program by comparison to the exact one-dimensional case. We have also calculated all the observables calculated in Ref. 8 and we agree completely. Our main interest is the calculation of the staggered spin-correlation function

$$G(\tau) = (-1)^{\tau_x + \tau_y} N^{-1} \sum_n \langle S_z(\mathbf{n}) S_z(\mathbf{n} + \boldsymbol{\tau}) \rangle.$$

We checked that the calculated correlation function satisfies the susceptibility sum rule.

We have performed calculations on lattices with sizes $10^2, 20^2,$ and 30^2 with periodic and open boundary conditions (BC). The number of iterations that we performed depends on the temperature and lattice size. For the higher temperatures and smaller lattices, we performed 0.5×10^6 iterations for thermalization, and 10^6 iterations for measurements. For the lower temperatures and bigger lattices longer runs were required for both thermalization and measurements. The quantities which required more iterations to reach equilibrium were r_1 , and the $G(\tau)$. For example, for the 20^2 lattice and at temperature $0.4J$ we performed 8×10^6 iterations for thermalization and 12×10^6 iterations for measurements. Simulations at lower temperatures or larger lattices are beyond realistic computational time scales.

We fitted the staggered G by the forms

$$\lim_{\tau \rightarrow \infty} G(\tau) = \begin{cases} A e^{-\tau/\xi(T)}, & \text{for open BC,} \\ A \cosh \left[\frac{\tau - L/2}{\xi(T)} \right], & \text{for periodic BC,} \end{cases} \quad (5)$$

where L is the size of the lattice. Figure 1(a) shows G

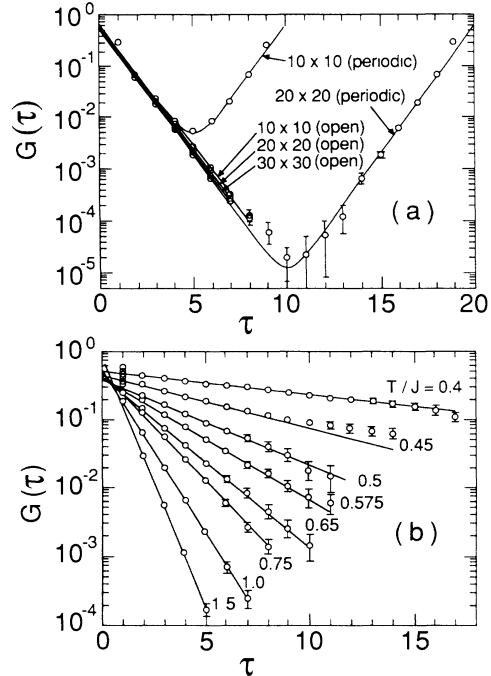


FIG. 1. (a) Staggered correlation function for lattices of size $10^2, 20^2,$ and 30^2 for $T=J$. (b) Correlation function for a 20^2 lattice at various temperatures. Error bars smaller than the diameter of the open circles are omitted.

calculated for the above three lattices for $T=J$ with periodic and open BC. The lines are obtained by our fitting all except the first few points of G by the forms of Eqs. (5). As may be observed in Fig. 1(a), G is approximated very well by Eqs. (5) for several orders of magnitude and the slopes are quite independent of the BC and finite-size effects. As T is lowered and the correlation length becomes comparable to the lattice size, the calculation of ξ requires larger lattices. We checked that the projected correlation function, $G_p(x) = (1/L) \sum_y G(x, y)$, gives the same correlations lengths within error bars. We found that open BC are more appropriate for the measurement of correlation lengths. In Fig. 1(b) we present G for our 20^2 lattice for various T . The correlations grow very rapidly in the range $1.0J-0.4J$, giving $\xi(J) = 0.9$ and $\xi(0.4J) = 13$.

In Fig. 2 we give an equilibrium configuration of clusters in the 20^2 lattice for $T=0.5J$ (top figure) where $\xi \sim 3.5$. The filled (open) circles denote up (down) spins. The clusters are drawn by solid lines. There is a large cluster involving most of the lattice sites and some other smaller ones. The lower part of Fig. 2 shows the clusters for 10^2 lattice and temperatures $0.4J$ (left-hand side) and $1.5J$ (right-hand side). In the $0.4J$ case we see almost a Néel configuration and only two clusters, one being monomer and another containing 99 sites. At $T=1.5J$ we have a rather disordered state with lots of small clusters.

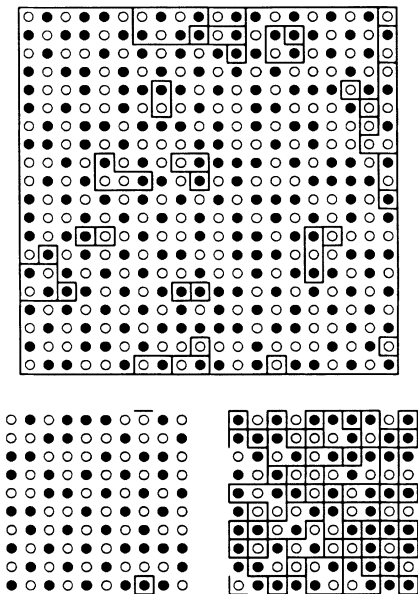


FIG. 2. Top: Clusters in a 20^2 lattice at equilibrium and at $T=J$. Bottom: Clusters in a 10^2 lattice at $T=0.4J$ (left-hand side) and at $T=1.5J$ (right-hand side). We only indicate one of the two possible spin states of the cluster.

The correlation length $\xi(T)$ is plotted in Fig. 3 on a logarithmic scale (see also Table I). The dashed line gives $\xi(T)$ obtained from the leading-order contribution to G at high temperatures $G(n)=(\beta J/4)^n$ and $\xi(T)=1/\ln(4T/J)$. Note that the agreement at high temperature is remarkable. In the range of temperatures $0.5J < T < 10J$ the numerical results are independent of lattice size. The behavior is clearly not linear; in fact, the slope $-d \ln \xi(T)/d(\ln T)$ increases rapidly with decreasing T and it is ~ 7 at $T=0.4J$.

Now we compare this behavior with existing theories. An exponential growth of the correlation length as a function of $1/T$ at low T is predicted by perturbative renormalization-group (PRG) theory⁹ of the classical Heisenberg model, giving $\xi(T)=A(T)e^{2\pi gJ/T}$, where the preexponential factor at low temperatures is $A(T)=CJ/T$. This form does not fit the data except in a small range of temperatures. Choosing this range to be $0.4J < T < 0.8J$ we obtain $C=0.18$ and $g=0.19$ and the fit is shown in Fig. 3 by the dashed-dotted line. This value of g is reduced from its classical value $g_{cl}=S^2$, which within PRG theory could be accounted for by quantum fluctuations. The fit is not very good which indicates either that the onset of the PRG behavior is at lower T or that nonperturbative effects such as topological configurations change the behavior of $\xi(T)$. A well known example is the XY model¹⁰ where a phase with topological order exists because of vortices. Topological excitations are known to exist in the 2D classical Heisenberg model¹¹ also. It is believed, however, that in the

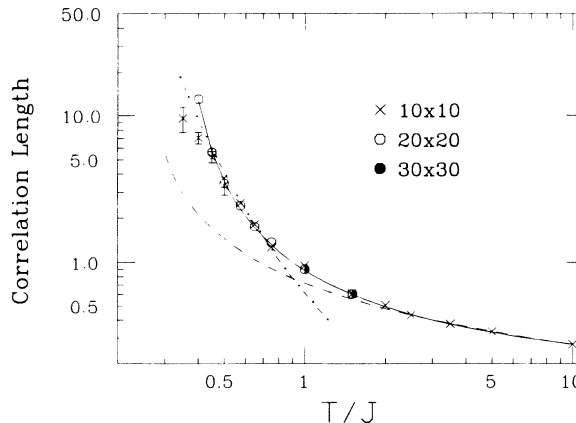


FIG. 3. Correlation length as a function of temperature for lattices of sizes 10^2 , 20^2 , and 30^2 and open BC. Error bars smaller than the diameter of the open circles are omitted. Dashed line is $\xi(T)=1/\ln(4T/J)$, the leading contribution at high T . Dashed-dotted and solid lines are as explained in the text.

classical model they do not alter the behavior predicted by PRG.⁹ In the quantum AFHM the structure of the ground state and the changes in $\xi(T)$ which such excitations may cause are theoretically unknown. We also tried to fit the correlation length by a Kosterlitz-Thouless¹⁰ form $\xi(T)=A \exp(B/|T-T_c|^\nu)$. The fit is good (solid line), giving $\nu=0.5$, the same as in the Kosterlitz-Thouless case, and $T_c=0.3J$ (and $A=0.178$, $B=1.338$). As a result of the Mermin-Wagner theorem,¹² the average staggered magnetization is zero at $T \neq 0$. However, the theorem does not exclude a transition to a phase where G decays algebraically ($\xi=\infty$) below some finite T_c because of topological order. This fit could be fortuitous; the reader, therefore, should take this *only* as an indication that topological instanton con-

TABLE I. The correlation length for various lattices and temperatures, and for open and periodic BC.

T	L=10		L=20		L=30
	Open	Periodic	Open	Periodic	Open
0.35	9.6(2.0)				
0.4	7.1(7)	11(6)	13.0(9)		
0.45	5.2(5)		5.6(4)		
0.5	3.3(5)	4.6(2.7)	3.4(3)		
0.575	2.6(2)	2.5(2)	2.4(2)		
0.65	1.82(8)	1.68(8)	1.74(6)		
0.75	1.27(3)	1.40(5)	1.36(8)	1.36(3)	
1	0.96(3)	0.92(2)	0.90(3)	0.88(2)	0.94(2)
1.5	0.611(8)	0.636(7)	0.61(1)	0.62(2)	0.60(1)
2	0.508(6)	0.507(7)			
2.5	0.434(3)	0.440(5)			
3.5	0.378(2)	0.386(5)			
5	0.333(2)	0.345(6)			
10	0.273(2)	0.265(7)			

figurations similar to those found in Ref. 11 might play an important role in our case.

Regardless of any theoretical interpretation, our results are consistent with the neutron-scattering data.⁴ The neutron- and Raman-scattering data give a value for the AF coupling of $J \approx 10^3$ K. In the neighborhood of room temperature, i.e., $\sim 0.3J$, a reasonable extrapolation gives correlation lengths of the order of those observed⁴ or higher. The average staggered magnetization at finite temperature in 2D is zero as expected.¹²

The three-dimensional (3D) AF ordering of $\text{La}_2\text{CuO}_{4-y}$ happens at a lower temperature scale than the AF coupling J . This can be explained as a result of both the weak layer coupling inherent in these materials and the special crystalline arrangement which tends to frustrate a 3D order. The orthorhombic distortion presumably relieves some frustration and produces three-dimensional Néel order at $T_N \sim 200$ K.

The authors are grateful to Dr. B. Berg, Dr. G. Bhanot, Dr. D. Duke, Dr. K. Huang, Dr. D. Petcher, Dr. Y.-L. Wang, and Dr. P. Weisz for useful discussions. This work was supported in part by the Florida State University (FSU) Supercomputer Computations Research Institute (SCRI) which is partially funded by the U. S. Department of Energy through Contract No. DE-FC05-85ER250000. A portion of the calculation was performed on the ETA-10 supercomputer at the FSU SCRI.

Note added.—While this work was in press we obtained the detailed behavior¹³ of the correlation length as a function of temperature. A detailed comparison with the data as well as implementation of 3D effects due to weak interlayer coupling (producing a Néel temperature $T_N \approx 200$ K) will be given elsewhere.¹⁴

¹J. G. Bednorz and K. A. Müller, *Z. Phys. B* **64**, 188 (1986); S. Uchida, H. Takagi, K. Katasawa, and S. Tanaka, *Jpn. J. Appl. Phys. Pt. 2* **26**, L1 (1987); C. W. Chu, P. H. Hor, R. L. Meng, L. Gao, Z. J. Huang, and Y. Q. Wang, *Phys. Rev. Lett.* **58**, 405 (1987); R. Cava, R. B. van Dover, B. Batlogg, and E. A. Rietman, *Phys. Rev. Lett.* **58**, 408 (1987).

²H. Thomann, P. Tindall, and D. C. Johnston, to be published.

³D. Vaknin, S. K. Sinha, D. E. Moncton, D. C. Johnston, J. M. Newsam, C. R. Safinya, and H. E. King, Jr., *Phys. Rev. Lett.* **58**, 2802 (1987).

⁴G. Shirane, Y. Endoh, R. J. Birgeneau, M. A. Kastner, Y. Hidaka, M. Oda, M. Suzuki, and T. Murakami, *Phys. Rev. Lett.* **59**, 1613 (1987).

⁵K. B. Lyons, P. A. Fleury, J. P. Remeika, A. S. Cooper, and T. J. Negran, *Phys. Rev. B* **37**, 2353 (1988).

⁶J. E. Hirsch, *Phys. Rev. Lett.* **54**, 1317 (1985); P. W. Anderson, G. Baskaran, Z. Zou, and T. Hsu, *Phys. Rev. Lett.* **58**, 2790 (1987); S. Kivelson, D. S. Rokhsar, and J. P. Sethna, *Phys. Rev. B* **35**, 8865 (1987); A. E. Ruckenstein, P. J. Hirschfeld, and J. Appel, *Phys. Rev. B* **36**, 857 (1987).

⁷K. Huang and E. Manousakis, *Phys. Rev. B* **36**, 8302 (1987); E. Kaxiras and E. Manousakis, *Phys. Rev. B* **37**, 656 (1988).

⁸D. H. Lee, J. D. Joannopoulos, and J. W. Negele, *Phys. Rev. B* **30**, 1599 (1984).

⁹S. H. Shenker and J. Tobochnik, *Phys. Rev. B* **22**, 4462 (1980).

¹⁰J. Kosterlitz and D. Thouless, *J. Phys. C* **6**, 1181 (1973); J. Kosterlitz, *J. Phys. C* **7**, 1046 (1974).

¹¹A. A. Belavin and A. M. Polyakov, *Pis'ma Zh. Eksp. Teor. Fiz.* **22**, 503 (1975) [*JETP Lett.* **22**, 245 (1975)].

¹²N. D. Mermin and H. Wagner, *Phys. Rev. Lett.* **22**, 1133 (1966).

¹³Y. Endoh *et al.*, to be published.

¹⁴E. Manousakis and R. Salvador, to be published.